Kinematics of Articulated Planar Linkages

Jing-Shan Zhao* and Song-Tao Wei

State Key Laboratory of Tribology, Department of Mechanical Engineering, Tsinghua University, Beijing, China

This paper proposes a kinematics algorithm in screw coordinates for articulated linkages. As the screw consists of velocity and position variables of a joint, the solutions of the forward and inverse velocities are the functions of position coordinates and their time derivatives. The most prominent merit of this kinematic algorithm is that we only need the first order numerical differential interpolation for computing the acceleration. To calculate the displacement, we also only need the first order numerical integral of the velocity. This benefit stems from the screw the coordinates of which are velocity components. Both the forward and the inverse kinematics have the similar calculation process in this method. Through examples of planar open-chain linkage, single closed-chain linkage and multiple closed-chain linkage, the kinematics algorithm is validated. It is particularly fit for developing numerical programmers for forward and inverse kinematics in the same procedures, including the velocity, displacement and acceleration which provide the fundamental information for dynamics of the linkage.

Keywords: kinematics, numerical algorithm, planar open-chain linkage, closed-chain linkage, articulated joint

INTRODUCTION

Kinematics of a linkage aims at studying its motion without regard to forces (Norton, 2004) for the synthesis of a mechanism (Suh and Radcliffe, 1978) or to accomplish the desired motion (Shigley and Uicher, 1980) and determine its rigid-body dynamic behavior (Bottema and Roth, 1979; Waldron and Kinematics, 2004). Kinematic geometry (Hunt, 1978), geometric design (McCarthy and Soh, 2011), theoretical kinematics of robotic mechanisms (McCarthy, 1990; Duffy, 1996; Davidson and Hunt, 2004; Dai, 2014), and the analysis, synthesis and optimization of spatial kinematic chains (Angeles, 1982) are elaborated in previous works in the past decades. Kinematic analysis of a linkage requires the algebraic equations that might be iterated numerically. Computational kinematic analysis plays a vital role in the study of a mechanical system (Saura et al., 2019). It is the most straightforward procedure for kinematics and dynamics to select the absolute coordinates of the reference point as the variables (García de Jalón and Bayo, 1994). This selection has the advantage of normally leading to a facilitated expression for the constraints and Jacobian matrices of a multi-body system (García de Jalón and Bayo, 1994). The forward kinematics of a serial linkage is easier than its inverse kinematics while the forward kinematics of a parallel linkage is more complex than its inverse kinematics (Suh and Radcliffe, 1978; Bottema and Roth, 1979; Duffy, 1980; Shigley and Uicher, 1980; Angeles, 1982; García de Jalón and Bayo, 1994; Duffy, 1996).

In the past half century, parallel manipulators witnessed very quick development. Parallel manipulators have been attracted a great attention ever since the industry application of Gough's tire testing machine and Stewart's platform for its superior performance over its serial counterparts in terms of loading capacity, rigidity and accuracy (Gough and Whitehall, 1962; Stewart, 1965). However, the forward kinematics usually contains a group of nonlinear algebraic

equations that are complexly coupled and there are no general methods to solve them analytically (Chapelle and Bidaud, 2004; Wu et al., 2009). It has been recognized as the general purpose of a software that standardized procedures should be proposed for reducing the kinematic analysis of mechanism to simplify the problem (Kong et al., 2016). Different procedures were developed to establish the restriction equations to solve their time derivatives of first and second orders (Zhao et al., 2016). Actually, such procedures can be accomplished through vector-loop processing for planar linkages (Brát and Lederer, 1973; Kong et al., 2018). The forward kinematics are either established in the functions of structure parameters and input variables numerically (Yang et al., 2018) or presented in algebraic coordinates (Wu et al., 2013; Kong et al., 2019). The inverse kinematic problem consists of finding the joint variables to achieve a desired configuration of a mechanism (Chapelle and Bidaud, 2004; Wu et al., 2013).

To understand the kinematic performance of a linkage, many scholars have been proposing different theories (McCarthy, 1990; Duffy, 1996; Davidson and Hunt, 2004; Dai, 2014; Zhao et al., 2016; Amiri and Mazaheri, 2020; Faghidian and Mohammad-Sedighi, 2020), methods (Angeles, 1982; Kong et al., 2018; Yang et al., 2018; Kong et al., 2019; Shen et al., 2020), algorithms (García de Jalón and Bayo, 1994; Kong et al., 2016; Saura et al., 2019) and software (Brát and Lederer, 1973; García de Jalón and Bayo, 1994; Wu et al., 2009; Wu et al., 2017). This paper focuses on an algorithm in the screw coordinates to solve the velocity of articulated planar linkage and investigates the displacement and acceleration. A screw is a line vector accompanied by a secondary vector attached with a pitch. As the geometrical element, a screw with six components plays a vital role in kinematics and mechanics of a mechanism (Barus, 1900). The paper develops an algorithm to analyze the displacement, velocity and acceleration of articulated planar mechanisms in twist coordinates of each joint. This is the first try to use screw coordinates to completely study the displacement, velocity and acceleration of linkages in a general systematic way. Because the kinematics analysis starts from the velocity, the solutions of forward and inverse kinematics of a mechanism have the same form in expression which facilitates the programming and calculation. The discussion is not restricted to the kinematics of revolute jointed planar linkages, and the similar principles also apply to spatial mechanisms.

INSTANTANEOUS TWIST OF THE END EFFECTOR OF A SERIES MECHANISM

Definition of Twist

Table 1 is the definition of parameters in this paper.

Figure 1A shows an articulated link AB that is rotating around a fixed revolute joint A with angular velocity of ω_A around the z-axis. The velocity of any point P attached to the rigid link AB can be expressed by $\boldsymbol{v}_P = \boldsymbol{\omega}_A \times \boldsymbol{r}_{AP}$. As a result, the velocity of point P on the extended rigid body of link AB that is overlapped with the origin of the coordinate frame is $\boldsymbol{v}_o = \boldsymbol{\omega}_A \times \boldsymbol{r}_{Ao}$ where $\boldsymbol{r}_{Ao} = -\boldsymbol{r}_A$ which is illustrated in **Figure 1B**.

TABLE 1 | Definition of parameters.

Parameters	Definition
$\boldsymbol{\omega}_A$	The relative angular velocity of joint A
$\boldsymbol{v}_P$	The velocity of any point P attached to the rigid link AB
$\boldsymbol{r}_A$	The vector direction of joint A
o	The screw of joint A
o	The unit screw of joint A
o	The screw of end effector
S	The screw matrix of end effector
$\boldsymbol{\omega}$	The vector of relative angular velocity

Also, there is $\boldsymbol{v}_o = \boldsymbol{\omega}_A \times (-\boldsymbol{r}_A) = \boldsymbol{r}_A \times \boldsymbol{\omega}_A$ which is illustrated in **Figure 1C**. The dual 3-dimensional vectors $\boldsymbol{\omega}_A$ and $\boldsymbol{v}_o$ can fully determine the rotation of link AB. So, a dual vector can be defined as

$$_o\$_A = \begin{bmatrix} \boldsymbol{\omega}_A \\ \boldsymbol{r}_A \times \boldsymbol{\omega}_A \end{bmatrix} \qquad (1)$$

where $_o\$_A$ is a screw that expresses the twist of link AB that is rotating around joint A with a marking point superimposing with the origin o of the coordinate system. Supposing that $\boldsymbol{e}_z = \begin{bmatrix} 0 & 0 & 1 \end{bmatrix}^T$, **Equation 1** can be rewritten as

$$_o\$_A = \omega_A \begin{bmatrix} \boldsymbol{e}_z \\ \boldsymbol{r}_A \times \boldsymbol{e}_z \end{bmatrix} \qquad (2)$$

where ω_A is the angular speed of the rotation about joint A. Let

$$_o\$_{Au} = \begin{bmatrix} \boldsymbol{e}_z \\ \boldsymbol{r}_A \times \boldsymbol{e}_z \end{bmatrix} \qquad (3)$$

where $o\$_{Au}$ is called unit screw because the norm of $\boldsymbol{e}_z$ is $\|\boldsymbol{e}_z\| = 1$ [35].

In **Equation 3**, the first three components indicate the unit direction of a rotation and the last three components present implicitly the position of the axis of rotation with respect to the origin of the coordinate system (Zhao et al., 2014). Therefore, **Equation 2** can be denoted by

$$_o\$_A = \omega_A {}_o\$_{Au} \qquad (4)$$

Twist Matrix of a Series Pivoted Kinematic Chain

When a second link BC is jointed with AB at B(see **Figure 2A**), the relative twist of BC with respect to AB can be analyzed by fixing AB with the ground which is indicated by **Figure 2B**.

With the similar procedure mentioned above, we get

$$_o\$_B = \omega_B {}_o\$_{Bu} \qquad (5)$$

where ω_B is the relative speed of link BC with respect to AB rotating around the revolute joint B, and

$$_o\$_{Bu} = \begin{bmatrix} \boldsymbol{e}_z \\ \boldsymbol{r}_B \times \boldsymbol{e}_z \end{bmatrix} \qquad (6)$$

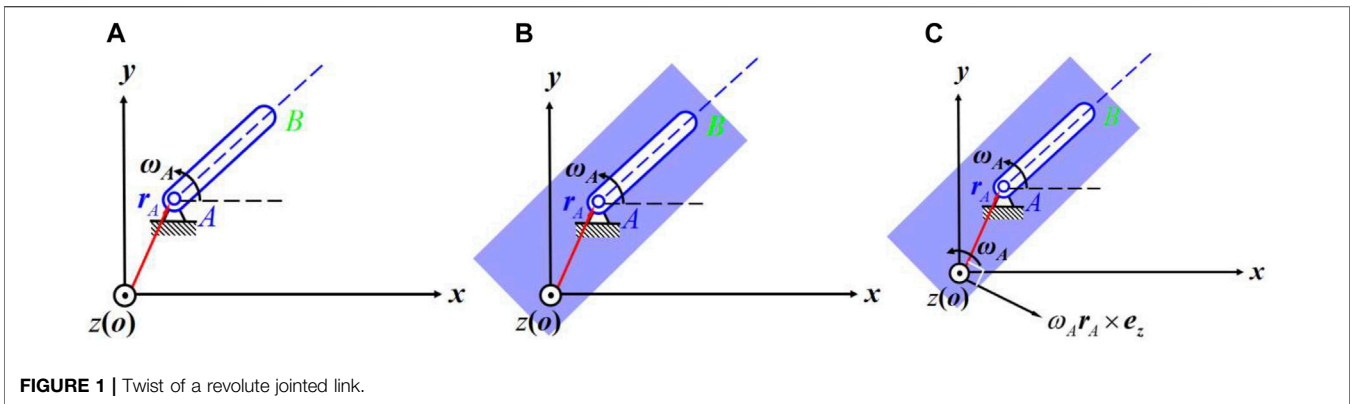According to the principle of linear superposition, the absolute angular velocity of link BC is (Zhao et al., 2014)
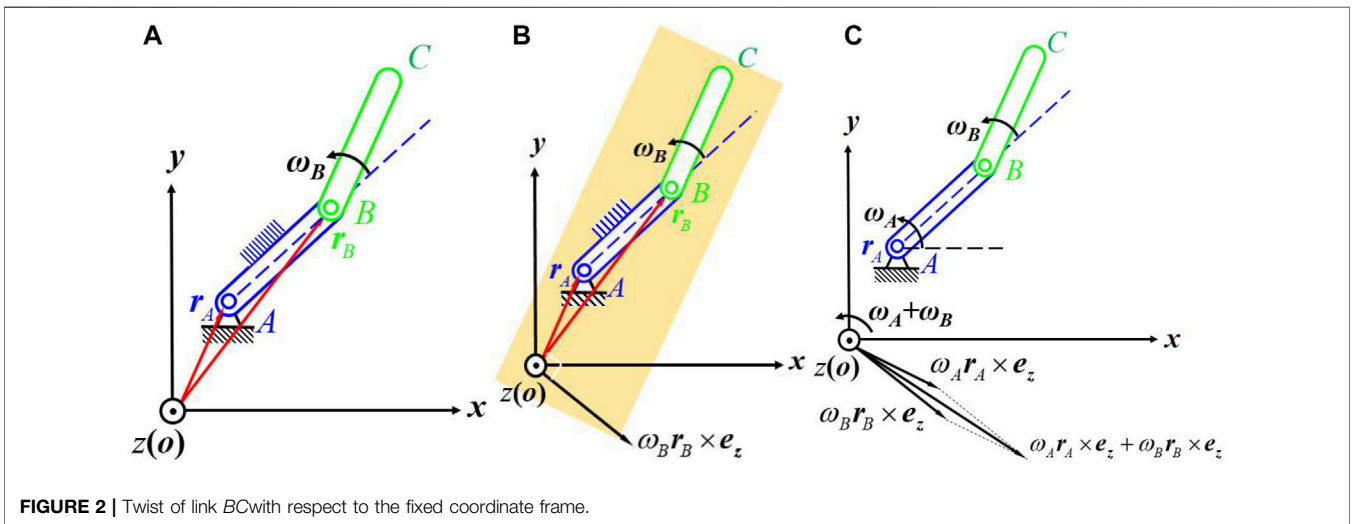
FIGURE 1 | Twist of a revolute jointed link.

FIGURE 2 | Twist of link BC with respect to the fixed coordinate frame.

$$\boldsymbol{\omega}_{BC} = \boldsymbol{\omega}_A + \boldsymbol{\omega}_B \qquad (7)$$

and the absolute velocity of link BC with the marking point that is superimposed with the origin at the moment is

$$_o\boldsymbol{v}_{Bc} = \omega_A\left(\boldsymbol{r}_A \times \boldsymbol{e}_z\right) + \omega_B\left(\boldsymbol{r}_B \times \boldsymbol{e}_z\right) \qquad (8)$$

where $_o\boldsymbol{v}_{BC}$ indicates the velocity of a point on link BC that is at this instant superimposed with the origin illustrated in **Figure 2C**.

As a result, the twist of link BC with respect to the coordinate system is

$$_o\$_{BC} = \begin{bmatrix} \boldsymbol{\omega}_{BC} \\ _o\boldsymbol{v}_{BC} \end{bmatrix} = \begin{bmatrix} \omega_A\boldsymbol{e}_z + \omega_B\boldsymbol{e}_z \\ \omega_A\boldsymbol{r}_A \times \boldsymbol{e}_z + \omega_B\boldsymbol{r}_B \times \boldsymbol{e}_z \end{bmatrix} \qquad (9)$$

Equation (9) can be rewritten as

$$_o\$_{BC} = \omega_A\ _o\$_{Au} + \omega_B\ _o\$_{Bu} \qquad (10)$$

which can be expressed in matrix multiplication form:

$$_o\$_{BC} = \mathbf{S}_{BC}\boldsymbol{\omega}_{BC} \qquad (11)$$

where $\mathbf{S}_{BC} = \begin{bmatrix} \boldsymbol{e}_z & \boldsymbol{e}_z \\ \boldsymbol{r}_A \times \boldsymbol{e}_z & \boldsymbol{r}_B \times \boldsymbol{e}_z \end{bmatrix}$ and $\boldsymbol{\omega}_{BC} = \begin{bmatrix} \omega_A \\ \omega_B \end{bmatrix}$.

Similarly, the twist of the end effector, denoted by $_o\$_E$, of a kinematic chain in series illustrated by **Figure 3** can be expressed as.

$$_o\$_E = \mathbf{S}\boldsymbol{\omega} \qquad (12)$$

where

$$\mathbf{S} = \begin{bmatrix} _o\$_1 & _o\$_2 & \cdots & _o\$_n \end{bmatrix} \qquad (13)$$

and

$$\boldsymbol{\omega} = \begin{bmatrix} \omega_1 & \omega_2 & \cdots & \omega_n \end{bmatrix}^T \qquad (14)$$

Eq. 13 is called the unit twist matrix of a serial linkage while **Equation 14** presents a vector including all relative angular speeds of each joint relative to its previous neighbor in the kinematic chain. Screw matrix 13) is made up of the geometry parameters of the mechanism. It can be programmed in the computer software. This procedure offers an explicit inference of kinematic attributes for velocities in the mechanisms that have the same topology.

KINEMATICS OF A REVOLUTE JOINTED MECHANISM WITH SERIAL OPEN CHAIN

From **Equation 12**, we know that the twist of the end effector with a marking point of the origin of the coordinate frame can be
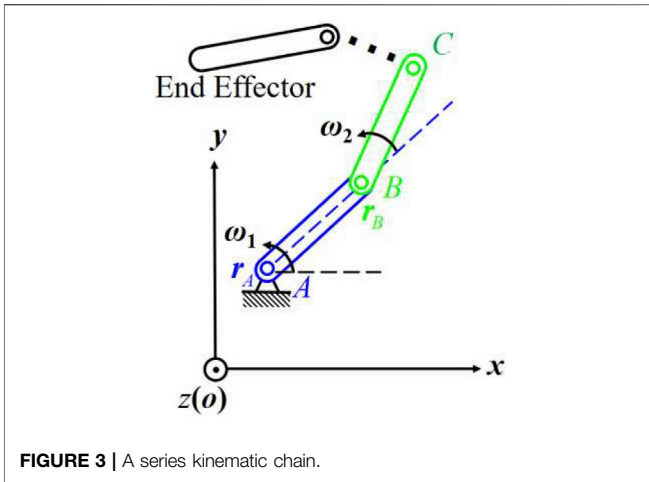
FIGURE 3 | A series kinematic chain.

directly obtained when ω_i ($i = 1, 2, \cdots n$) are all prescribed. Denote the twist by

$$_o\$_E = \begin{bmatrix} \boldsymbol{\omega}_E \\ _o\boldsymbol{v}_E \end{bmatrix} \tag{15}$$

We know that $\boldsymbol{\omega}_E$ is the absolute angular velocity of the end effector and $\boldsymbol{v}_E (o)$ is the velocity of the point attached with the end effector that is superimposed with the origin of the coordinate system at this moment. The velocity of the geometry center of the end effector is therefore denoted by

$$_C\boldsymbol{v}_E = {}_o\boldsymbol{v}_E + \boldsymbol{\omega}_E \times \boldsymbol{r}_C \tag{16}$$

where $\boldsymbol{r}_C$ is the position vector of the geometry center of the end effector in the absolute ground coordinate system. As a result, we get the twist of the end effector at its central coordinate frame whose axes are parallel with the corresponding absolute ones at this instant:

$$_C\$_E = \begin{bmatrix} \boldsymbol{\omega}_E \\ _C\boldsymbol{v}_E \end{bmatrix} = \begin{bmatrix} \boldsymbol{\omega}_E \\ _o\boldsymbol{v}_E + \boldsymbol{\omega}_E \times \boldsymbol{r}_C \end{bmatrix} \tag{17}$$

where $\boldsymbol{\omega}_E$ is the absolute angular velocity of the end effector and $_C\boldsymbol{v}_E$ is the absolute linear velocity of the center of the end effector. **Eq. 17** is the forward kinematics of a serial linkage in screw form which provides all necessary parameters for developing the dynamics of the linkage.

After knowing the twist of the end effector with a marking point of the origin o of the coordinate frame, we can left multiply $\mathbf{S}^T$ at both sides of **Equation 15**:

$$\mathbf{S}^T\mathbf{S}\boldsymbol{\omega} = \mathbf{S}^T{}_o\$_E \tag{18}$$

where $\mathbf{S}^T$ is the transpose of matrix $\mathbf{S}$.

When $|\mathbf{S}^T(o)\mathbf{S}(o)| = 0$, the serial linkage is either redundantly actuated or in its singularity configuration. Otherwise, we get:

$$\boldsymbol{\omega} = \left[\mathbf{S}^T\mathbf{S}\right]^{-1}\mathbf{S}^T{}_o\$_E \tag{19}$$

where $\left[\mathbf{S}^T\mathbf{S}\right]^{-1}\mathbf{S}^T$ is called the pseudo inverse of the unit twist matrix $\mathbf{S}$. **Eq. 19** represents the inverse kinematics for the serial mechanism.

Figure 4 shows a planar linkage in series. In the absolute coordinate system, we gain the twist of the end effector:

$$_o\$_E = \mathbf{S}\boldsymbol{\omega} \tag{20}$$

where

$$\mathbf{S} = \begin{bmatrix} 0 & 0 & 1 & y_1 & -x_1 & 0 \\ 0 & 0 & 1 & y_2 & -x_2 & 0 \\ 0 & 0 & 1 & y_3 & -x_3 & 0 \end{bmatrix}^T \tag{21}$$

and

$$\boldsymbol{\omega} = \begin{bmatrix} \omega_1 & \omega_2 & \omega_3 \end{bmatrix}^T \tag{22}$$

Supposing the length of the links are l_1, l_2 and l_3, the coordinates of each revolute joint can be expressed by $x_1 = 0$, $y_1 = 0$, $x_2 = l_1 \cos\varphi_1$, $y_2 = l_1 \sin\varphi_1$, $x_3 = l_1 \cos\varphi_1 + l_2 \cos(\varphi_1 + \varphi_2)$, $y_3 = l_1 \sin\varphi_1 + l_2 \sin(\varphi_1 + \varphi_2)$, respectively. So the unit twist matrix 18) is

$$\mathbf{S} = \begin{bmatrix} 0 & 0 & 0 \\ 0 & 0 & 0 \\ 1 & 1 & 1 \\ 0 & l_1 \sin\varphi_1 & l_1 \sin\varphi_1 + l_2 \sin(\varphi_1 + \varphi_2) \\ 0 & -l_1 \cos\varphi_1 & -l_1 \cos\varphi_1 - l_2 \cos(\varphi_1 + \varphi_2) \\ 0 & 0 & 0 \end{bmatrix} \tag{23}$$

In accordance to **Equation 17**, we know that the twist of the end effector with the marking point on its center is

$$_C\$_E = \begin{bmatrix} \boldsymbol{\omega}_E \\ _C\boldsymbol{v}_E \end{bmatrix} = \begin{bmatrix} \boldsymbol{\omega}_1 + \boldsymbol{\omega}_2 + \boldsymbol{\omega}_3 \\ _o\boldsymbol{v}_E + (\boldsymbol{\omega}_1 + \boldsymbol{\omega}_2 + \boldsymbol{\omega}_3) \times \boldsymbol{r}_C \end{bmatrix} \tag{24}$$

where $\boldsymbol{r}_C = \begin{bmatrix} l_1 \cos\varphi_1 + l_2 \cos(\varphi_1 + \varphi_2) + \dfrac{1}{2}l_3 \cos(\varphi_1 + \varphi_2 + \varphi_3) \\ l_1 \sin\varphi_1 + l_2 \sin(\varphi_1 + \varphi_2) + \dfrac{1}{2}l_3 \sin(\varphi_1 + \varphi_2 + \varphi_3) \\ 0 \end{bmatrix}$.

By programming with the numerical algorithms, we obtain the forward kinematics of the linkage. With the initial conditions of $\varphi_1(0)$, $\varphi_2(0)$ and $\varphi_3(0)$, and ω_1, ω_2 and ω_3, we get the first set of parameters, $\boldsymbol{\omega}(1)$ from equation (22). And then we gain the first twist of the end effector from equation (20) and $\mathbf{S}(1)$ from equation (23) and $c\$_E(1)$ from equation (24)

Then we get the successive parameters of $\mathbf{S}(i)$ from **Equation 23** and $c\$_E(i)$ from **Equation 24** by updating the data:

$$\begin{cases} \varphi_1(i) = \varphi_1(0) + i\Delta t\omega_1 \\ \varphi_2(i) = \varphi_2(0) + i\Delta t\omega_2 \\ \varphi_3(i) = \varphi_3(0) + i\Delta t\omega_3 \end{cases} \tag{25}$$

where $i = 1, 2, \cdots$ and Δt is a finite small time increment. The absolute angular displacement of the end effector is

$$\varphi_E(i) = \varphi_1(i) + \varphi_2(i) + \varphi_3(i) \tag{26}$$

The angular accelerations of each joint can be numerically calculated by

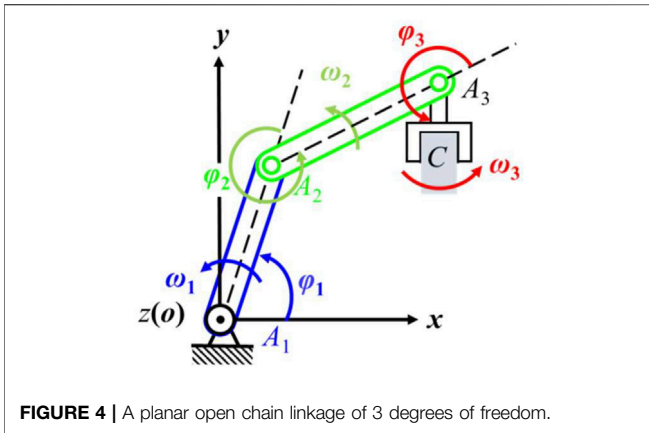$$\alpha_j(i) = \frac{\omega_j(i+1) - \omega_j(i-1)}{2\Delta t} \tag{27}$$

FIGURE 4 | A planar open chain linkage of 3 degrees of freedom.

where $j = 1, 2, \cdots, n$ represents the jth joint.

In forward kinematic, we let the angular velocity of screw joint O_1 be $3 \sin \pi t$, the angular velocity of screw joint O_2 be $2 \sin \frac{3\pi t}{2}$, the angular velocity of screw joint O_3 be $\sin 2 \pi t$ with the structure parameters and initial conditions in **Table 2**, we programmed the above process in MATLAB and drew the forward displacement, velocity and acceleration for each joint (see **Figure 5**) by numerical methods based on **Equations 25–27**.

KINEMATICS OF PIVOTED LINKAGES OF CLOSED CHAIN

Kinematics of the 4-bar Linkage

Figure 6 1) shows a planar 4-bar linkage in series and 2) a 4-bar mechanism with closed loop. The twist of the end effector of the 4-bar linkage in series can be gained from **Equation 12**:

$$_o\$_E = \mathbf{S}\boldsymbol{\omega}$$

where $\mathbf{S} = [\ \$_1 \quad \$_2 \quad \$_3 \quad \$_4\ ]$, $\boldsymbol{\omega} = [\ \omega_1 \quad \omega_2 \quad \omega_3 \quad \omega_4\ ]^T$ and $\$_1 = [0 \ 0 \ 1 \ y_1 \ -x_1 \ 0]^T$, $\$_2 = [0 \ 0 \ 1 \ y_2 \ -x_2 \ 0]^T$, $\$_3 = [0 \ 0 \ 1 \ y_3 \ -x_3 \ 0]^T$, $\$_4 = [0 \ 0 \ 1 \ y_4 \ -x_4 \ 0]^T$.

Eq. 12 indicates that the kinematic chain forms a closed loop when the end effector is fixed with the frame (see **Figure 6B**). And therefore, there must be

$$_o\$_E = 0 \tag{28}$$

Eq. 28 is called the loop equation of the mechanism which can be used to solve all angular velocities by taking other known conditions into account. In the coordinate frame shown in **Figure 6**, $x_1 = 0$, $y_1 = 0$, $x_2 = l_1 \cos \varphi_1$, $y_2 = l_1 \sin \varphi_1$, $x_3 = l_1 \cos \varphi_1 + l_2 \cos (\varphi_1 + \varphi_2)$, $y_3 = l_1 \sin \varphi_1 + l_2 \sin (\varphi_1 + \varphi_2)$, $x_4 = l_1 \cos \varphi_1 + l_2 \cos (\varphi_1 + \varphi_2) + l_3 \cos (\varphi_1 + \varphi_2 + \varphi_3)$ and $y_4 = l_1 \sin \varphi_1 + l_2 \sin (\varphi_1 + \varphi_2) + l_3 \sin (\varphi_1 + \varphi_2 + \varphi_3)$, we get that

$$o\$_E = \begin{bmatrix} 0 \\ 0 \\ o\$_E (3, 1) \\ o\$_E (4, 1) \\ o\$_E (5, 1) \\ 0 \end{bmatrix} = \begin{bmatrix} 0 \\ 0 \\ 0 \\ 0 \\ 0 \\ 0 \end{bmatrix} \tag{29}$$

where $o\$_E (3, 1) = \omega_1 + \omega_2 + \omega_3 + \omega_4$, $o\$_E (4, 1) = \omega_2 l_1 \sin \varphi_1 + \omega_3 [l_1 \sin \varphi_1 + l_2 \sin (\varphi_1 + \varphi_2)] + \omega_4 [l_1 \sin \varphi_{11} + l_2 \sin (\varphi_1 + \varphi_2) + l_3 \sin (\varphi_1 + \varphi_2 + \varphi_3)]$, $o\$_E (5, 1) = -\omega_2 l_1 \cos \varphi_1 - \omega_3 [l_1 \cos \varphi_1 + l_2 \cos (\varphi_1 + \varphi_2)] - \omega_4 [l_1 \cos \varphi_1 + l_2 \cos (\varphi_1 + \varphi_2) + l_3 \cos (\varphi_1 + \varphi_2 + \varphi_3)]$.

Rearranging equation (29) presents

$$\begin{cases} \omega_2 + \omega_3 + \omega_4 = -\omega_1 \\ \omega_2 l_1 \sin \varphi_1 + \omega_3 [l_1 \sin \varphi_1 + l_2 \sin (\varphi_1 + \varphi_2)] + \omega_4 [l_1 \sin \varphi_1 \\ \quad + l_2 \sin (\varphi_1 + \varphi_2) + l_3 \sin (\varphi_1 + \varphi_2 + \varphi_3)] = 0 \\ -\omega_2 l_1 \cos \varphi_1 - \omega_3 [l_1 \cos \varphi_1 + l_2 \cos (\varphi_1 + \varphi_2)] - \omega_4 [l_1 \cos \varphi_1 \\ \quad + l_2 \cos (\varphi_1 + \varphi_2) + l_3 \cos (\varphi_1 + \varphi_2 + \varphi_3)] = 0 \end{cases}$$

Therefore, we gain the forward kinematics of the closed-chain 4-bar linkage (**Figure 6B**):

$$\boldsymbol{\omega}_F = \mathbf{A}^{-1} \boldsymbol{v}_1 \tag{30}$$

where

$$\mathbf{A} = \begin{bmatrix} 1 & 1 & 1 \\ l_1 \sin \varphi_1 & l_1 \sin \varphi_1 + l_2 \sin (\varphi_1 + \varphi_2) & l_1 \sin \varphi_1 + l_2 \sin (\varphi_1 + \varphi_2) + l_3 \sin (\varphi_1 + \varphi_2 + \varphi_3) \\ -l_1 \cos \varphi_1 & -l_1 \cos \varphi_1 - l_2 \cos (\varphi_1 + \varphi_2) & -l_1 \cos \varphi_1 - l_2 \cos (\varphi_1 + \varphi_2) - l_3 \cos (\varphi_1 + \varphi_2 + \varphi_3) \end{bmatrix},$$

$$\boldsymbol{\omega}_F = \begin{bmatrix} \omega_2 \\ \omega_3 \\ \omega_4 \end{bmatrix} \text{ and } \boldsymbol{v}_1 = \begin{bmatrix} -\omega_1 \\ 0 \\ 0 \end{bmatrix}.$$

When the output of ω_4 is known, we can also get that

$$\begin{cases} \omega_1 + \omega_2 + \omega_3 = -\omega_4 \\ \omega_2 l_1 \sin \varphi_1 + \omega_3 [l_1 \sin \varphi_1 + l_2 \sin (\varphi_1 + \varphi_2)] \\ \quad = -\omega_4 [l_1 \sin \varphi_1 + l_2 \sin (\varphi_1 + \varphi_2) + l_3 \sin (\varphi_1 + \varphi_2 + \varphi_3)] \\ -\omega_2 l_1 \cos \varphi_1 - \omega_3 [l_1 \cos \varphi_1 + l_2 \cos (\varphi_1 + \varphi_2)] \\ \quad = \omega_4 [l_1 \cos \varphi_1 + l_2 \cos (\varphi_1 + \varphi_2) + l_3 \cos (\varphi_1 + \varphi_2 + \varphi_3)] \end{cases}$$

Consequently, the inverse kinematics of the 4 bar mechanism is now rewritten as
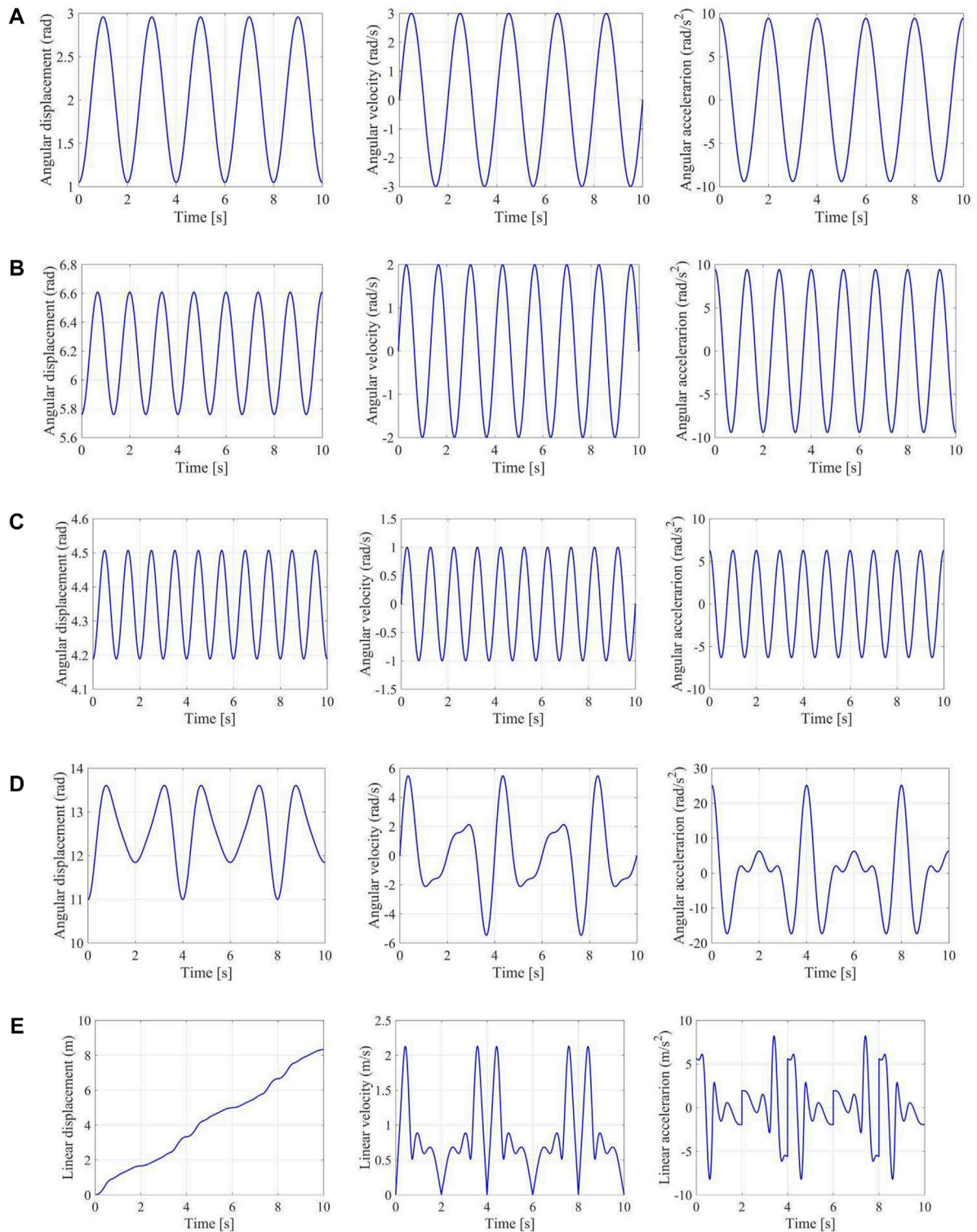
$$\boldsymbol{\omega}_I = \mathbf{B}^{-1} \boldsymbol{v}_4 \tag{31}$$

where $\mathbf{B} = \begin{bmatrix} 1 & 1 & 1 \\ 0 & l_1 \sin \varphi_1 & l_1 \sin \varphi_1 + l_2 \sin (\varphi_1 + \varphi_2) \\ 0 & -l_1 \cos \varphi_1 & -l_1 \cos \varphi_1 - l_2 \cos (\varphi_1 + \varphi_2) \end{bmatrix}$,

$$\boldsymbol{\omega}_I = \begin{bmatrix} \omega_1 \\ \omega_2 \\ \omega_3 \end{bmatrix} \text{ and } \boldsymbol{v}_4 = \begin{bmatrix} -\omega_4 \\ -\omega_4 [l_1 \sin \varphi_1 + l_2 \sin (\varphi_1 + \varphi_2) + l_3 \sin (\varphi_1 + \varphi_2 + \varphi_3)] \\ \omega_4 [l_1 \cos \varphi_1 + l_2 \cos (\varphi_1 + \varphi_2) + l_3 \cos (\varphi_1 + \varphi_2 + \varphi_3)] \end{bmatrix}.$$

TABLE 2 | Structure parameters and initial conditions.

	$\varphi_2 (0) (rad)$	$\varphi_3 (0) (rad)$	ω_{A_1} (rad/s)	ω_{A_2} (rad/s)	ω_{A_3} (rad/s)	l_1 (mm)	l_2 (mm)	l_3 (mm)
	$\frac{\pi}{3}$	$\frac{11\pi}{6}$	$\frac{4\pi}{3}$	$3 \sin \pi t$	$2 \sin \frac{3\pi t}{2}$	$\sin 2 \pi t$	200	210	300

FIGURE 5 | Forward kinematics of a planar 4-bar mechanism. (A) Angular displacement, velocity and acceleration of joint A_1; (B) Angular displacement, velocity and acceleration of joint A_2; (C) Angular displacement, velocity and acceleration of joint A_3; (D) Angular displacement, velocity and acceleration of end effector; (E) Linear velocity and acceleration of the center of end effector.
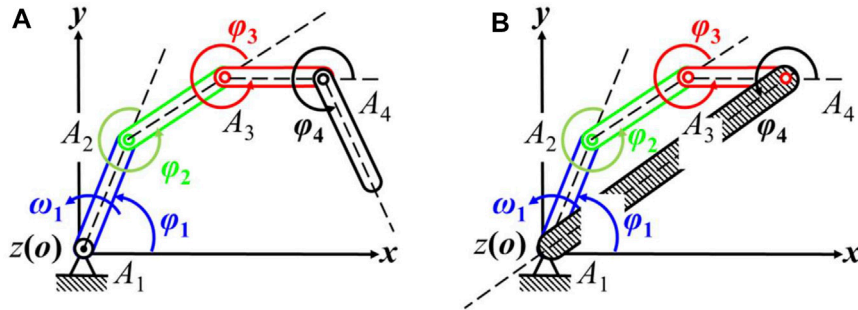
FIGURE 6 | Planar 4-bar linkages. **(A)** A 4-bar linkage in series; **(B)** A 4-bar linkage with closed loop.

In this regard, the forward velocity and inverse velocity have the same form in mathematical expressions which is one of the advantages of this algorithm. Then, we get the successive parameters of $\boldsymbol{\omega}_F$ from **Equation 30** or $\boldsymbol{\omega}_I$ from **Equation 31** by updating the data of $\mathbf{A}$, $\mathbf{B}$ and $\boldsymbol{v}_4$ with the interactions below:

$$\begin{cases} \varphi_1(i+1) = \varphi_1(i) + \Delta t \omega_1(i) \\ \varphi_2(i+1) = \varphi_2(i) + \Delta t \omega_2(i) \\ \varphi_3(i+1) = \varphi_3(i) + \Delta t \omega_3(i) \end{cases} \tag{32}$$

where $i = 1, 2, \cdots$ represents the ith iteration and Δt is a finite small time increment.

Compared with the Denavit-Hartenberg notation for a closed loop (Craig, 1986), the kinematics algorithm in screw form here only requires to implement one numerical integration 32) for displacement and one numerical differential 27) for acceleration in the absolute coordinate frame. This provides a more convergent algorithm to develop computational kinematics of a linkage. We let the angular velocity of joint O_1 is 2 rad/s and with the structure parameters and initial conditions in **Table 3**, we programmed the method in MATLAB and obtained the forward displacement, velocity and acceleration for each joint (see **Figure 7**) by numerical methods based on **Equations 32**, **27** for validating the method.

Kinematics of an Articulated Linkage of 1 degree of Freedom With Multiple Closed Chains

Figure 8 illustrates a planar multi-closed-chain 6-bar linkage 1) in which there are two independent closed chains (b). For the first closed chain of a 4-bar linkage (**Figure 8** (c)), the loop equation can be found from **Equation 27**:

$$\begin{bmatrix} 0 & 0 & 0 & 0 \\ 0 & 0 & 0 & 0 \\ 1 & 1 & 1 & 1 \\ y_{A_1} & y_{A_2} & y_{A_3} & y_{A_4} \\ -x_{A_1} & -x_{A_2} & -x_{A_3} & -x_{A_4} \\ 0 & 0 & 0 & 0 \end{bmatrix} \begin{bmatrix} \omega_{A_1} \\ \omega_{A_2} \\ \omega_{A_3} \\ \omega_{A_4} \end{bmatrix} = 0$$

where $\underline{\omega_{A_1}}$ is the input. Rearranging this loop equation yields:

$$\begin{bmatrix} 1 & 1 & 1 \\ y_{A_2} & y_{A_3} & y_{A_4} \\ -x_{A_2} & -x_{A_3} & -x_{A_4} \end{bmatrix} \begin{bmatrix} \omega_{A_2} \\ \omega_{A_3} \\ \omega_{A_4} \end{bmatrix} = \begin{bmatrix} -\underline{\omega_{A_1}} \\ -\underline{\omega_{A_1}}\, y_{A_1} \\ \underline{\omega_{A_1}}\, x_{A_1} \end{bmatrix} \tag{33}$$

Similarly, we get the loop equation of the second coupled 5-bar closed chain linkage (**Figure 8** (d)) from **Equation 28**:

$$\begin{bmatrix} 0 & 0 & 0 & 0 & 0 \\ 0 & 0 & 0 & 0 & 0 \\ 1 & 1 & 1 & 1 & 1 \\ y_{A_1} & y_{A_2} & y_{B_1} & y_{B_2} & y_{B_3} \\ -x_{A_1} & -x_{A_2} & -x_{B_1} & -x_{B_2} & -x_{B_3} \\ 0 & 0 & 0 & 0 & 0 \end{bmatrix} \begin{bmatrix} \omega_{A_1} \\ \omega_{A_2} \\ \omega_{B_1} \\ \omega_{B_2} \\ \omega_{B_3} \end{bmatrix} = 0$$

Rearranging this loop equation presents:

$$\begin{bmatrix} 1 & 1 & 1 & 1 \\ y_{A_2} & y_{B_1} & y_{B_2} & y_{B_3} \\ -x_{A_2} & -x_{B_1} & -x_{B_2} & -x_{B_3} \end{bmatrix} \begin{bmatrix} \omega_{A_2} \\ \omega_{B_1} \\ \omega_{B_2} \\ \omega_{B_3} \end{bmatrix} = \begin{bmatrix} -\omega_{A_1} \\ -\omega_{A_1}\, y_{A_1} \\ \underline{\omega_{A_1}}\, x_{A_1} \end{bmatrix} \tag{34}$$

So the forward kinematics of the multiple closed chain linkage can be obtained by associating these double-loop **Equations 33**, **34**:

$$\boldsymbol{\omega} = \mathbf{M}^{-1} \boldsymbol{v} \tag{35}$$

where $\mathbf{M} = \begin{bmatrix} 1 & 1 & 1 & 0 & 0 & 0 \\ y_{A_2} & y_{A_3} & y_{A_4} & 0 & 0 & 0 \\ -x_{A_2} & -x_{A_3} & -x_{A_4} & 0 & 0 & 0 \\ 1 & 0 & 0 & 1 & 1 & 1 \\ y_{A_2} & 0 & 0 & y_{B_1} & y_{B_2} & y_{B_3} \\ -x_{A_2} & 0 & 0 & -x_{B_1} & -x_{B_2} & -x_{B_3} \end{bmatrix}$,

$\boldsymbol{\omega} = \begin{bmatrix} \omega_{A_2} \\ \omega_{A_3} \\ \omega_{A_4} \\ \omega_{B_1} \\ \omega_{B_2} \\ \omega_{B_3} \end{bmatrix}$ and $\boldsymbol{v} = \begin{bmatrix} -\omega_{A_1} \\ -\omega_{A_1}\, y_{A_1} \\ \underline{\omega_{A_1}}\, x_{A_1} \\ -\underline{\omega_{A_1}} \\ -\omega_{A_1}\, y_{A_1} \\ \underline{\omega_{A_1}}\, x_{A_1} \end{bmatrix}$.

TABLE 3 | Structure parameters and initial conditions.

$\varphi_1(0)$ (rad)	$\underline{\omega_{A_1}}$ (rad/s)	l_1 (mm)	l_2 (mm)	l_3 (mm)	l_4 (mm)	y_{A_4} (mm)
$\frac{\pi}{6}$	2	100	150	200	210	0
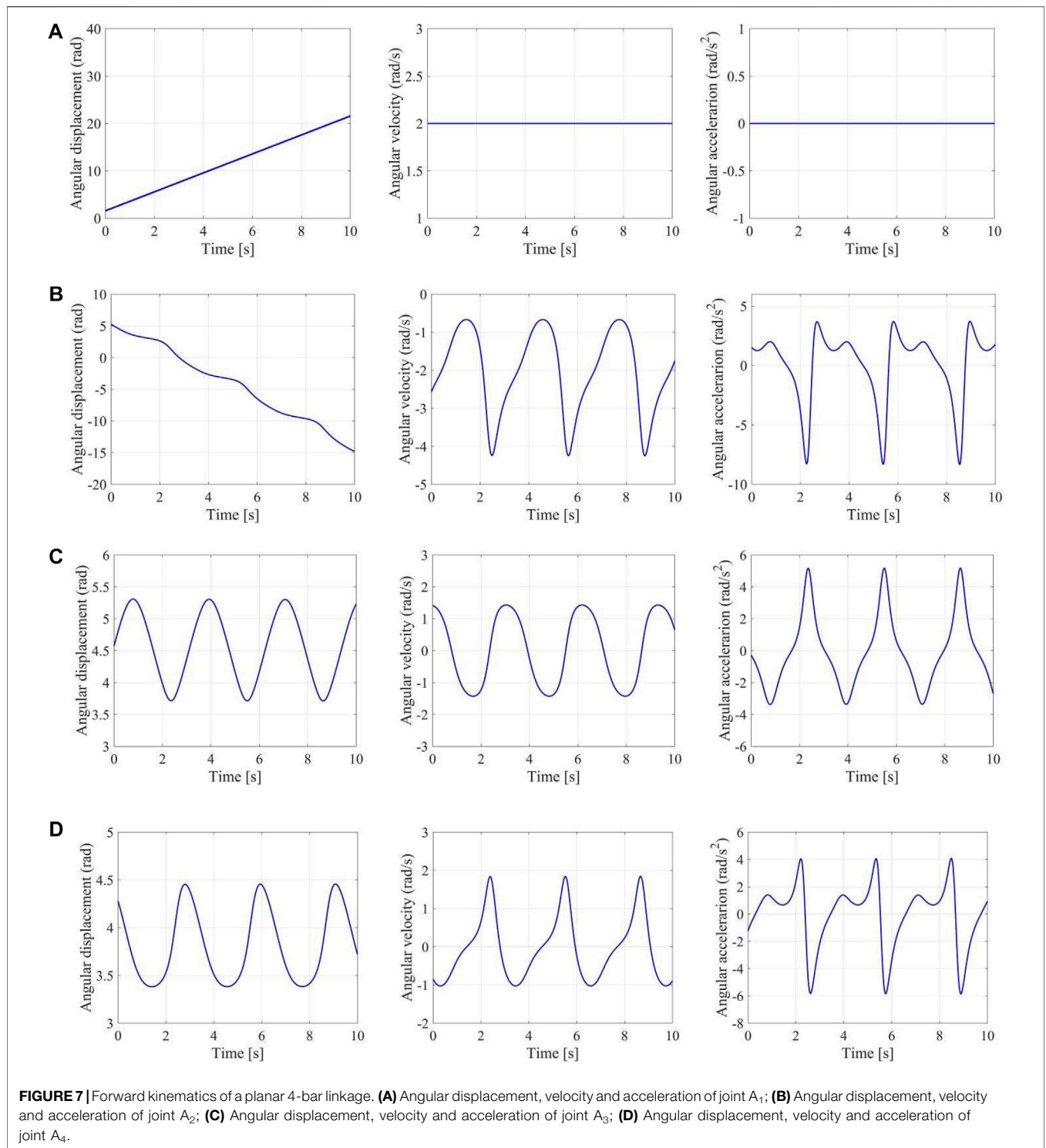
FIGURE 7 | Forward kinematics of a planar 4-bar linkage. **(A)** Angular displacement, velocity and acceleration of joint A_1; **(B)** Angular displacement, velocity and acceleration of joint A_2; **(C)** Angular displacement, velocity and acceleration of joint A_3; **(D)** Angular displacement, velocity and acceleration of joint A_4.

We let the angular velocity of joint O_1 is 2 rad/s and with the structure parameters and initial conditions in **Table 4**, we programmed the method in MATLAB and gained the forward displacement, velocity and acceleration for each joint (see **Figure 9**) by numerical methods with **Equation 35**.

Kinematics of a Planar Mechanism of More Degrees of Freedom With Single Closed Chain

Figure 10 illustrates 1) a planar 5-bar linkage in series and 2) a 5-bar linkage of closed loop. The twist of the end
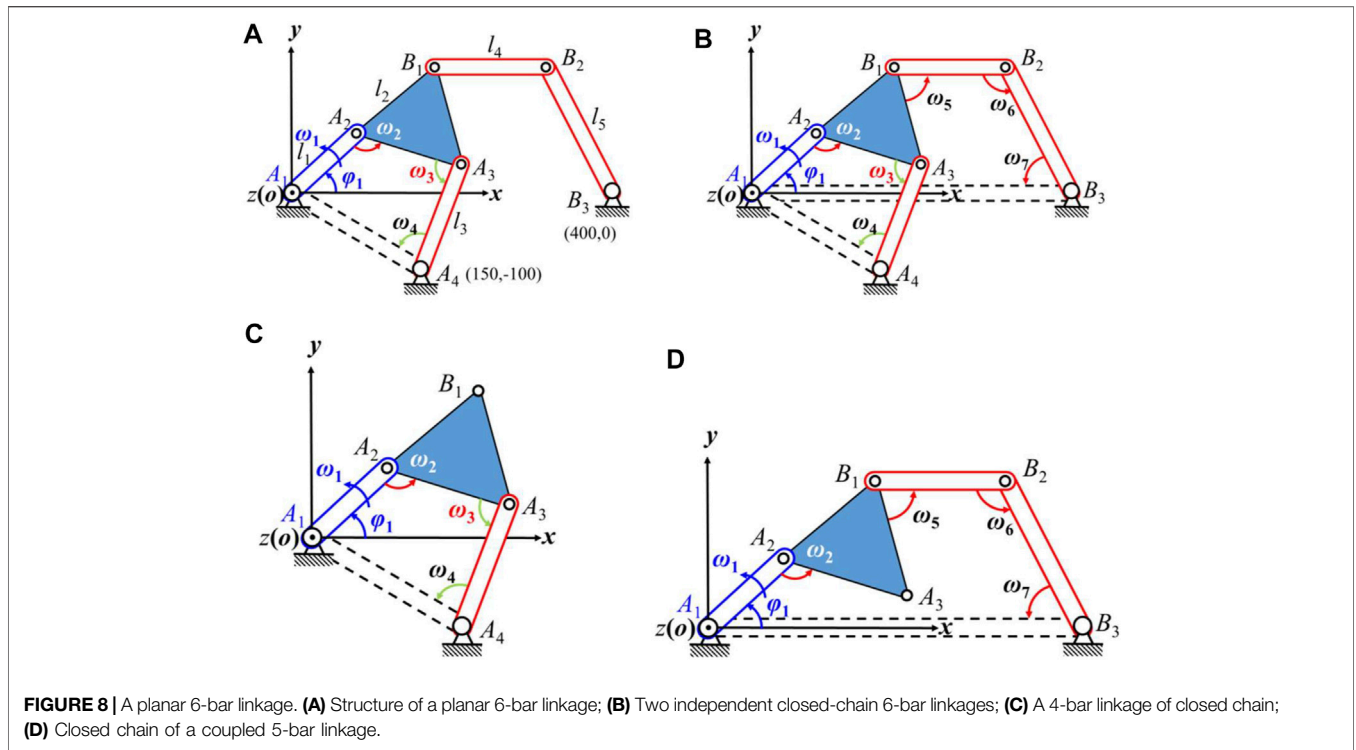
FIGURE 8 | A planar 6-bar linkage. (A) Structure of a planar 6-bar linkage; (B) Two independent closed-chain 6-bar linkages; (C) A 4-bar linkage of closed chain; (D) Closed chain of a coupled 5-bar linkage.

effector of the 5-bar linkage in series can be gained by **Equation 12**:

$$_o\$_E = \mathbf{S}\boldsymbol{\omega}$$

where $\mathbf{S} = [\ \$_1 \ \$_2 \ \$_3 \ \$_4 \ \$_5 \ ]$, $\boldsymbol{\omega} = [\omega_1 \ \omega_2 \ \omega_3 \ \omega_4 \ \omega_5]^T$ and $\$_1 = [0 \ 0 \ 1 \ y_1 \ -x_1 \ 0]^T$, $\$_2 = [0 \ 0 \ 1 \ y_2 \ -x_2 \ 0]^T$, $\$_3 = [0 \ 0 \ 1 \ y_3 \ -x_3 \ 0]^T$, $\$_4 = [0 \ 0 \ 1 \ y_4 \ -x_4 \ 0]^T$, $\$_5 = [0 \ 0 \ 1 \ y_5 \ -x_5 \ 0]^T$.

From **Equation 12**, we know that the kinematic chain forms a closed loop when the end effector is fixed with the frame (**Figure 10B**). Therefore, there must be $_o\$_E = 0$. In the coordinate frame shown in **Figure 10**, $x_1 = 0$, $y_1 = 0$, $x_2 = l_1 \cos\varphi_1$, $y_2 = l_1 \sin\varphi_1$, $x_3 = l_1 \cos\varphi_1 + l_2 \cos(\varphi_1 + \varphi_2)$, $y_3 = l_1 \sin\varphi_1 + l_2 \sin(\varphi_1 + \varphi_2)$, $x_4 = l_1 \cos\varphi_1 + l_2 \cos(\varphi_1 + \varphi_2) + l_3 \cos(\varphi_1 + \varphi_2 + \varphi_3)$, $y_4 = l_1 \sin\varphi_1 + l_2 \sin(\varphi_1 + \varphi_2) + l_3 \sin(\varphi_1 + \varphi_2 + \varphi_3)$, and $x_5 = l_1 \cos\varphi_1 + l_2 \cos(\varphi_1 + \varphi_2) + l_3 \cos(\varphi_1 + \varphi_2 + \varphi_3) + l_4 \cos(\varphi_1 + \varphi_2 + \varphi_3 + \varphi_4)$, and $y_5 = l_1 \sin\varphi_1 + l_2 \sin(\varphi_1 + \varphi_2) + l_3 \sin(\varphi_1 + \varphi_2 + \varphi_3) + l_4 \sin(\varphi_1 + \varphi_2 + \varphi_3 + \varphi_4)$, we get that

$$o\$_E = \begin{bmatrix} 0 \\ 0 \\ \omega_1 + \omega_2 + \omega_3 + \omega_4 + \omega_5 \\ \omega_2 l_1 \sin\varphi_1 + \omega_3[l_1 \sin\varphi_1 + l_2 \sin(\varphi_1 + \varphi_2)] \\ +\omega_4[l_1 \sin\varphi_1 + l_2 \sin(\varphi_1 + \varphi_2) + l_3 \sin(\varphi_1 + \varphi_2 + \varphi_3)] \\ +\omega_5[l_1 \cos\varphi_1 + l_2 \cos(\varphi_1 + \varphi_2) + l_3 \cos(\varphi_1 + \varphi_2 + \varphi_3) \\ +l_4 \cos(\varphi_1 + \varphi_2 + \varphi_3 + \varphi_4)] \\ -\omega_2 l_1 \cos\varphi_1 - \omega_3[l_1 \cos\varphi_1 + l_2 \cos(\varphi_1 + \varphi_2)] \\ -\omega_4[l_1 \cos\varphi_1 + l_2 \cos(\varphi_1 + \varphi_2) + l_3 \cos(\varphi_1 + \varphi_2 + \varphi_3)] \\ -\omega_5[l_1 \cos\varphi_1 + l_2 \cos(\varphi_1 + \varphi_2) + l_3 \cos(\varphi_1 + \varphi_2 + \varphi_3) \\ +l_4 \cos(\varphi_1 + \varphi_2 + \varphi_3 + \varphi_4)] \\ 0 \end{bmatrix} = \begin{bmatrix} 0 \\ 0 \\ 0 \\ 0 \\ 0 \\ 0 \end{bmatrix} \quad (36)$$

Then there is

$$\begin{cases} \omega_2 + \omega_3 + \omega_4 = -\omega_1 - \omega_5 \\ \omega_2 l_1 \sin\varphi_1 + \omega_3[l_1 \sin\varphi_1 + l_2 \sin(\varphi_1 + \varphi_2)] \\ \quad + \omega_4 \begin{bmatrix} l_1 \sin\varphi_1 + l_2 \sin(\varphi_1 + \varphi_2) \\ +l_3 \sin(\varphi_1 + \varphi_2 + \varphi_3) \end{bmatrix} \\ \quad = -\omega_5 \begin{bmatrix} l_1 \sin\varphi_1 + l_2 \sin(\varphi_1 + \varphi_2) \\ +l_3 \sin(\varphi_1 + \varphi_2 + \varphi_3) \\ +l_4 \sin(\varphi_1 + \varphi_2 + \varphi_3 + \varphi_4) \end{bmatrix} \\ \quad - \omega_2 l_1 \cos\varphi_1 - \omega_3[l_1 \cos\varphi_1 + l_2 \cos(\varphi_1 + \varphi_2)] \\ \quad - \omega_4 \begin{bmatrix} l_1 \cos\varphi_1 + l_2 \cos(\varphi_1 + \varphi_2) \\ +l_3 \cos(\varphi_1 + \varphi_2 + \varphi_3) \end{bmatrix} \\ \quad = \omega_5 \begin{bmatrix} l_1 \cos\varphi_1 + l_2 \cos(\varphi_1 + \varphi_2) \\ +l_3 \cos(\varphi_1 + \varphi_2 + \varphi_3) \\ +l_4 \cos(\varphi_1 + \varphi_2 + \varphi_3 + \varphi_4) \end{bmatrix} \end{cases}$$

Therefore, we get the forward kinematics of the closed-chain 5-bar linkage (**Figure 10B**):

$$\boldsymbol{\omega}_F = \mathbf{A}^{-1} \boldsymbol{\omega}_1 \quad (37)$$

where

$$\mathbf{A} = \begin{bmatrix} 1 & 1 & 1 \\ l_1 \sin\varphi_1 & l_1 \sin\varphi_1 + l_2 \sin(\varphi_1 + \varphi_2) & l_1 \sin\varphi_1 + l_2 \sin(\varphi_1 + \varphi_2) + l_3 \sin(\varphi_1 + \varphi_2 + \varphi_3) \\ -l_1 \cos\varphi_1 & -l_1 \cos\varphi_1 - l_2 \cos(\varphi_1 + \varphi_2) & -l_1 \cos\varphi_1 - l_2 \cos(\varphi_1 + \varphi_2) - l_3 \cos(\varphi_1 + \varphi_2 + \varphi_3) \end{bmatrix} \quad \boldsymbol{\omega}_F = \begin{bmatrix} \omega_2 \\ \omega_3 \\ \omega_4 \end{bmatrix}$$

and $\boldsymbol{\omega}_1 = \begin{bmatrix} -\omega_1 - \omega_5 & -\omega_5 \begin{bmatrix} l_1 \sin\varphi_1 + l_2 \sin(\varphi_1 + \varphi_2) \\ +l_3 \sin(\varphi_1 + \varphi_2 + \varphi_3) \\ +l_4 \sin(\varphi_1 + \varphi_2 + \varphi_3 + \varphi_4) \end{bmatrix} & \omega_5 \begin{bmatrix} l_1 \cos\varphi_1 + l_2 \cos(\varphi_1 + \varphi_2) \\ +l_3 \cos(\varphi_1 + \varphi_2 + \varphi_3) \\ +l_4 \cos(\varphi_1 + \varphi_2 + \varphi_3 + \varphi_4) \end{bmatrix} \end{bmatrix}^T$.

Eq. 37 represents the forward velocity of the planar 5-bar mechanism of 2 degrees of freedom. In accordance to the numerical **Eq. 32**, **27**, we obtain the forward displacement and

TABLE 4 | Structure parameters and initial conditions.

$\varphi_1(0)\,(\text{rad})$	$\underline{\omega_{A_1}}\,(\text{rad/s})$	$l_1\,(\text{mm})$	$l_2\,(\text{mm})$	$l_3\,(\text{mm})$	$l_4\,(\text{mm})$	$l_5\,(\text{mm})$	$x_{B_3}\,(\text{mm})$	$y_{B_3}\,(\text{mm})$	$x_{A_4}\,(\text{mm})$	$y_{A_4}\,(\text{mm})$
$\frac{\pi}{4}$	2	100	150	200	210	300	400	0	150	−100
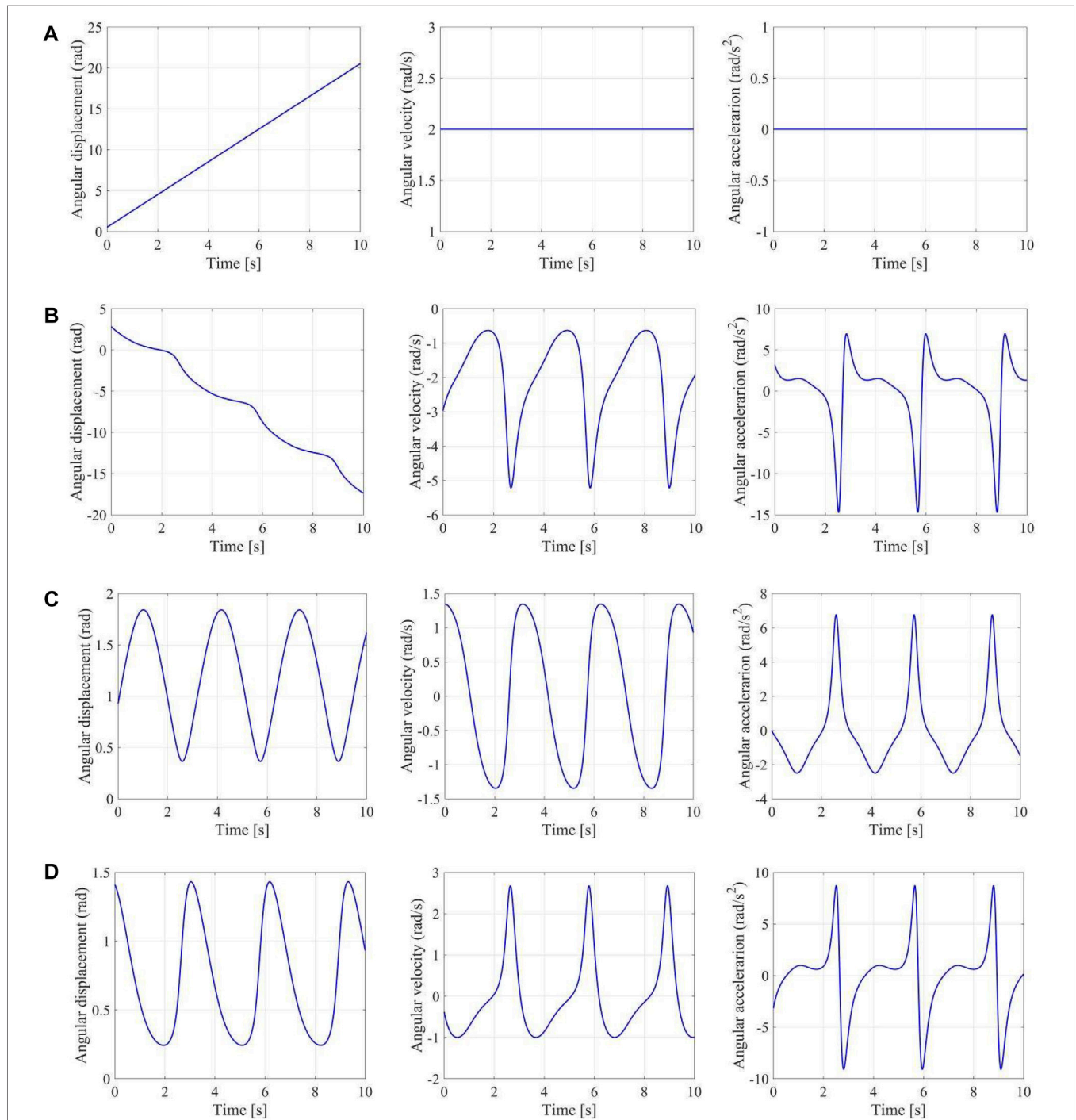
FIGURE 9 | Forward kinematics of a multiple closed chain linkage. **(A)** Angular displacement, velocity, and acceleration of joint A_1; **(B)** Angular displacement, velocity, and acceleration of joint A_2; **(C)** Angular displacement, velocity, and acceleration of joint A_3; **(D)** Angular displacement, velocity, and acceleration of joint A_4; **(E)** Angular displacement, velocity, and acceleration of joint B_1; **(F)** Angular displacement, velocity, and acceleration of joint B_2; **(G)** Angular displacement, velocity, and acceleration of joint B_3.
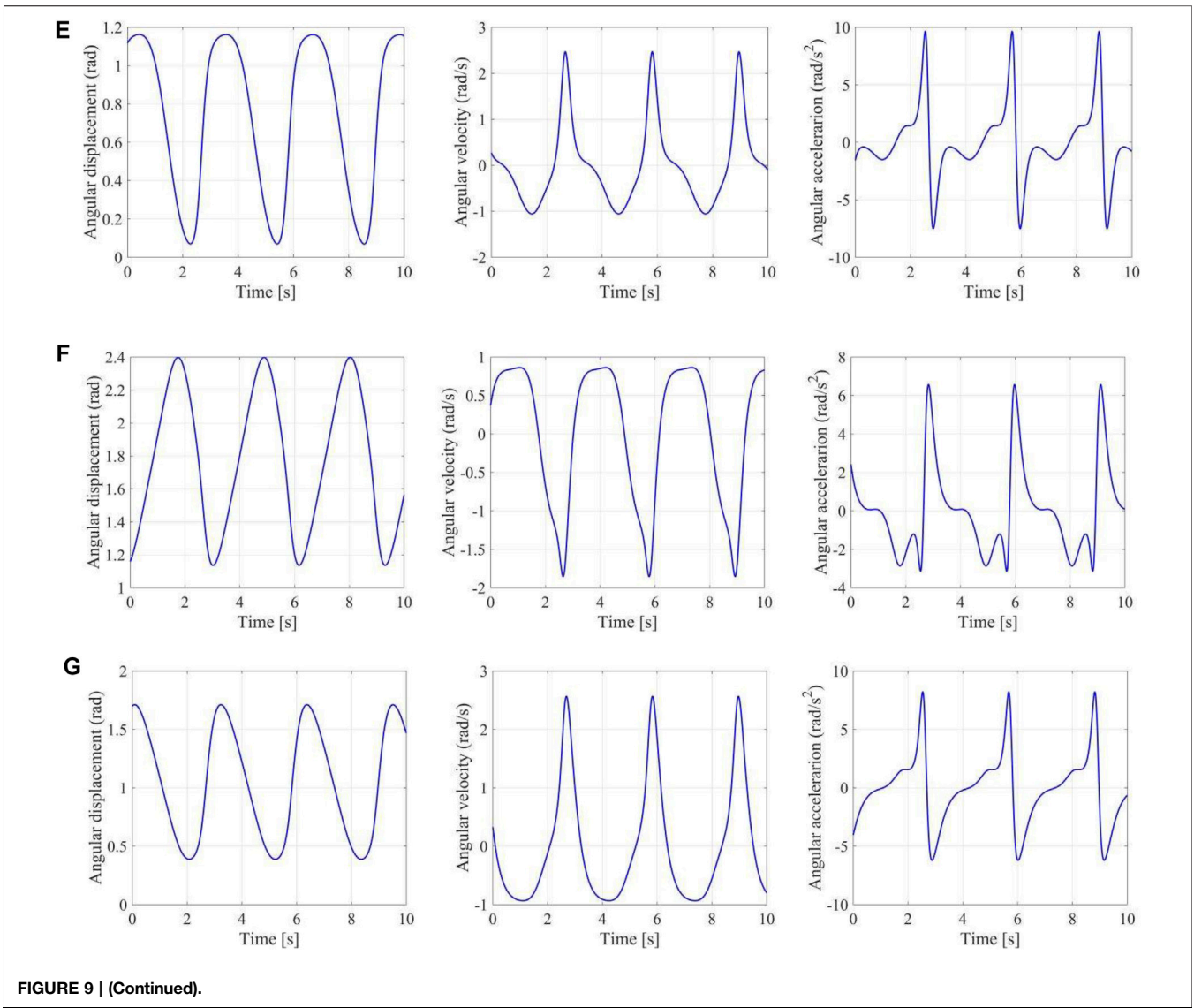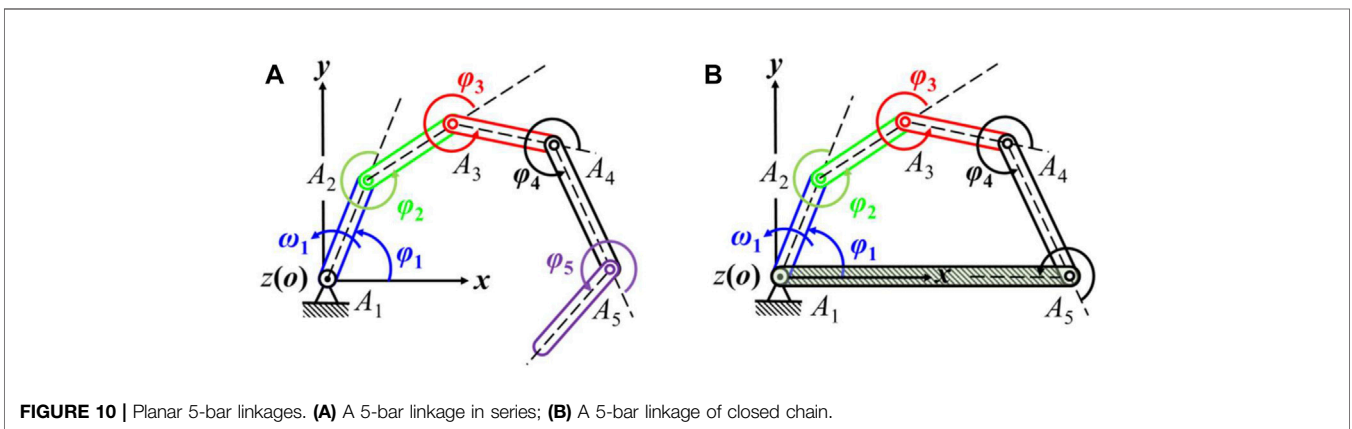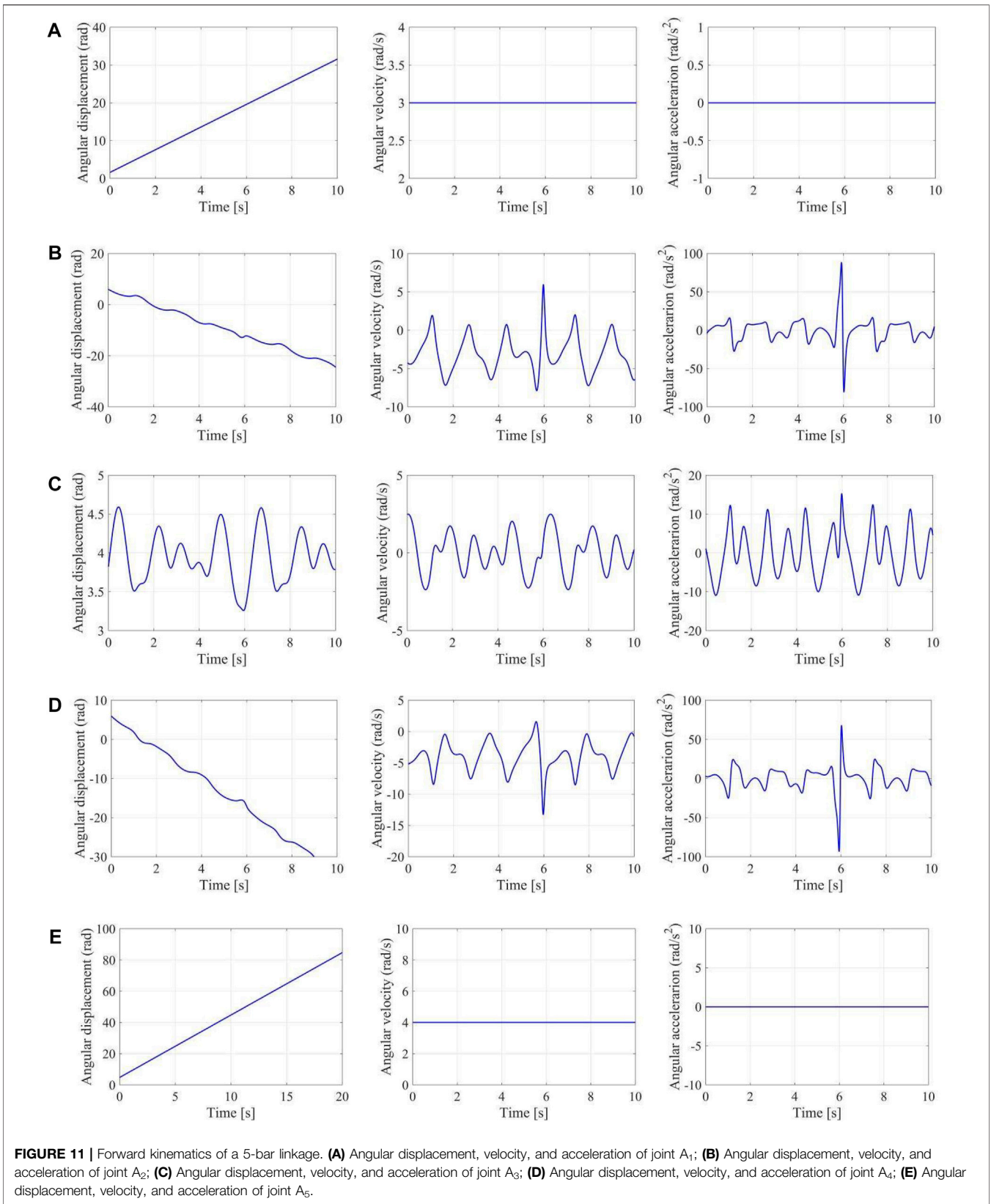
FIGURE 9 | (Continued).

FIGURE 10 | Planar 5-bar linkages. (A) A 5-bar linkage in series; (B) A 5-bar linkage of closed chain.

TABLE 5 | Initial conditions and structure parameters.

$\varphi_1(0)\,(\text{rad})$	$\varphi_5(0)\,(\text{rad})$	$\underline{\omega_{A_1}}\,(\text{rad/s})$	$\underline{\omega_{A_5}}\,(\text{rad/s})$	$l_1\,(\text{mm})$	$l_2\,(\text{mm})$	$l_3\,(\text{mm})$	$l_4\,(\text{mm})$	$l_5\,(\text{mm})$	$x_{A_5}\,(\text{mm})$	$y_{A_5}\,(\text{mm})$
$\frac{\pi}{4}$	$\frac{5\pi}{3}$	3	4	100	300	300	100	200	400	0

FIGURE 11 | Forward kinematics of a 5-bar linkage. (A) Angular displacement, velocity, and acceleration of joint A_1; (B) Angular displacement, velocity, and acceleration of joint A_2; (C) Angular displacement, velocity, and acceleration of joint A_3; (D) Angular displacement, velocity, and acceleration of joint A_4; (E) Angular displacement, velocity, and acceleration of joint A_5.

acceleration of the mechanism with a single closed chain. We let the angular velocity of joint O_1 is 3 rad/s, the angular velocity of joint O_2 is 4 rad/s, and with the structure parameters in **Table 5**, the displacement, velocity and acceleration curves for each joint are illustrated in **Figure 11** by numerical formulas of **Eq. 32**, **27** in accordance to **Equation 37**.

CONCLUSION

This paper proposed a method to investigate the displacement, velocity and acceleration of a mechanism in screw coordinates in a general systematic way. As the twist of an articulated rigid body includes the angular velocity and linear velocity, the corresponding displacements of all joints are obtained through one-order integration of the velocity solutions and the accelerations are represented by the first order numerical differential interpolation. Compared to the traditional methods in which the displacement parameters are the only variables that will surely lead to the second order differential interpolations for the accelerations, the advantages of this method is that both the forward and inverse kinematics of a mechanism can be expressed in a same way and only one-order differential interpolation is needed to get the acceleration and one-order integral is required to calculate the displacement. This method is validated by planar mechanisms in series, single closed loop and multiple closed loops. This method is particularly suitable for programming the computational software for forward and inverse kinematics of a mechanism, covering the velocity, displacement and acceleration. Although this paper discusses the kinematics of revolute jointed planar

mechanisms, the same principles may apply to any spatial linkages.

DATA AVAILABILITY STATEMENT

The original contributions presented in the study are included in the article/**Supplementary Material**, further inquiries can be directed to the corresponding author.

AUTHOR CONTRIBUTIONS

methodology, J-SZ; software, S-TW; validation, J-SZ, S-TW; formal analysis, J-SZ; investigation, J-SZ, S-TW; resources, J-SZ; data curation, S-TW; writing—original draft preparation, J-SZ; writing—review and editing, J-SZ, S-TW; visualization, J-SZ, S-TW; supervision, J-SZ; project administration, J-SZ; funding acquisition, J-SZ All authors have read and agreed to the published version of the manuscript.

FUNDING

SUPPLEMENTARY MATERIAL

The Supplementary Material for this article can be found online at: https://www.frontiersin.org/articles/10.3389/fmech.2021.774814/full#supplementary-material

REFERENCES

Amiri, A., and Mazaheri, H. (2020). Study on the Behavior of a Temperature-Sensitive Hydrogel Micro-channel via FSI and Non-FSI Approaches. *Acta Mech.* 231, 2799–2813. doi:10.1007/s00707-020-02673-z

Angeles, J. (1982). *Spatial Kinematic Chains: Analysis, Synthesis, and Optimization.* Berlin: Springer-Verlag, 55–76.

Barus, C. (1900). *A Treatise on the Theory of Screws.* Cambridge: Cambridge University Press, 1001–1003. doi:10.1126/science.12.313.1001

Bottema, O., and Roth, B. (1979). *Theoretical Kinematics.* New York, Jan: North-Holland, 35–56.

Brát, V., and Lederer, P. (1973). KIDYAN: Computer-Aided Kinematic and Dynamic Analysis of Planar Mechanisms. *Mechanism Machine Theor.* 8 (4), 457–467. doi:10.1016/0094-114X(73)90020-7

Chapelle, F., and Bidaud, P. (2004). Closed Form Solutions for Inverse Kinematics Approximation of General 6R Manipulators. *Mechanism Machine Theor.* 39 (3), 323–338. doi:10.1016/j.mechmachtheory.2003.09.003

Craig, J. (1986). *Introduction to Robotics, Mechanics and Control.* New York, Jan: Addison-Wesley, 33–137.

Dai, J. (2014). *Screw Algebra and Lie Groups and Lie Algebras.* 2nd Edition. Beijing: Higher Education Press, 123–140.

Davidson, J. K., and Hunt, K. H. (2004). *Robots and Screw Theory: Applications of Kinematics and Statics to Robotics.* New York: Oxford University Press, 56–78.

Duffy, J. (1980). *Analysis of Mechanisms and Robot Manipulators.* London: Edward Arnold, 123–135.

Duffy, J. (1996). *Statics and Kinematics with Applications to Robotics.* New York: Cambridge University Press, 46–78.

Faghidian, S. A., and Mohammad-Sedighi, H. (2020). Dynamics of Nonlocal Thick Nano-Bars. *Eng. Comput.* doi:10.1007/s00366-020-01216-3

García de Jalón, J., and Bayo, E. (1994). *Kinematic and Dynamic Simulation of Multibody Systems: The Real-Time Challenge.* New York, Jan: Springer-Verlag, 220–254.

Gough, V. E., and Whitehall, S. G. (1962). "Universal Tyre Test Machine," *Proceedings of the International Technical Congress FISITA.* UK: Institution of Mechanical Engineers, 117.

Hunt, K. H. (1978). *Kinematic Geometry of Mechanisms.* New York, Jan: Oxford University Press, 66–85.

Kong, K., Chen, G., and Hao, G. (2019). Kinetostatic Modeling and Optimization of a Novel Horizontal-Displacement Compliant Mechanism. *J. Mech. Robotics* 11 (6), 1. doi:10.1115/1.4044334

Kong, X., He, X., and Li, D. (2018). A Double-Faced 6R Single-Loop Overconstrained Spatial Mechanism. *J. Mech. robotics* 10 (3). 031013 doi:10.1115/1.4039224

Kong, X., Yu, J., and Li, D. (2016). Reconfiguration Analysis of a Two Degrees-Of-Freedom 3-4R Parallel Manipulator with Planar Base and Platform1. *J. Mech. Robotics* 8 (17). 011019 doi:10.1115/1.4031027

McCarthy, J. M. (1990). *An Introduction to Theoretical Kinematics.* London, Mar: The MIT Press, 33–45.

McCarthy, J. M., and Soh, G. S. (2011). *Geometric Design of Linkages.* New York, Jan: Springer, 13–46.

Norton, R. L. (2004). *Design of Machinery—An Introduction to the Synthesis and Analysis of Mechanisms and Machines.* 3rd ed. New York, Jan: McGraw-Hill Companies, Inc., 30–81.

Saura, M., Segado, P., and Dopico, D. (2019). Computational Kinematics of Multibody Systems: Two Formulations for a Modular Approach Based on Natural Coordinates. *Mechanism Machine Theor.* 142 (12). 103602 doi:10.1016/j.mechmachtheory.2019.103602

Shen, H., Chablat, D., Zeng, B., Li, J., Wu, G., and Yang, T.-L. (2020). A Translational Three-Degrees-Of-Freedom Parallel Mechanism with Partial Motion Decoupling and Analytic Direct Kinematics. *J. Mech. Robotics* 12 (2). 021112 doi:10.1115/1.4045972

Shigley, J. E., and Uicher, J. J. (1980). *Theory of Machines and Mechanisms*. New York, Jan: McGraw-Hill Companies, Inc.

Stewart, D. (1965). A Platform with Six Degrees of freedom. *Proc. Inst. Mech. Eng.* 180 (1), 371–386. doi:10.1243/pime_proc_1965_180_029_02

Suh, C. H., and Radcliffe, C. W. (1978). *Kinematics and Mechanisms Design*. New York: Wiley

Waldron, K. J., and Kinematics, G. L. Kinzel. (2004). *Dynamics, and Design of Machinery*. Hamilton PrintingNew York: John Wiley & Sons, 5–16.

Wu, J., Gao, Y., Zhang, B., and Wang, L. (2017). Workspace and Dynamic Performance Evaluation of the Parallel Manipulators in a spray-painting Equipment. *Robotics and Computer-Integrated Manufacturing* 44 (4), 199–207. doi:10.1016/j.rcim.2016.09.002

Wu, J., Li, T., Wang, J., and Wang, L. (2013). Performance Analysis and Comparison of Planar 3-DOF Parallel Manipulators with One and Two Additional Branches. *J. Intell. Robot Syst.* 72 (1), 73–82. doi:10.1007/s10846-013-9824-8

Wu, J., Wang, J., Wang, L., and Li, T. (2009). Dynamics and Control of a Planar 3-DOF Parallel Manipulator with Actuation Redundancy. *Mechanism and Machine TheoryApr* 44 (4), 835–849. doi:10.1016/j.mechmachtheory.2008.04.002

Yang, T.-L., Liu, A., Shen, H., Hang, L., and Jeffery Ge, Q. (2018). Composition Principle Based on Single-Open-Chain Unit for General Spatial Mechanisms and its Application-In Conjunction with a Review of Development of Mechanism Composition Principles. *J. Mech. Robotics* 10 (5). 051005 doi:10.1115/1.4040488

Zhao, D.-J., Zhao, J.-S., and Yan, Z.-F. (2016). Planar Deployable Linkage and its Application in Overconstrained Lift Mechanism. *J. Mech. Robotics* 8 (29). 021022 doi:10.1115/1.4032096

Zhao, J., Feng, Z., Chu, F., and Ma, N. (2014). *Advanced Theory of Constraint and Motion Analysis for Robot Mechanisms*. Elsevier, 113–157. doi:10.1016/B978-0-12-420162-0.00014-X10.1016/b978-0-12-420162-0.00004-7Free Motion of the End Effector of a Robot Mechanism